

Tunnelling coefficients across an arbitrary potential barrier

This article has been downloaded from IOPscience. Please scroll down to see the full text article.

2000 J. Phys. A: Math. Gen. 33 5449

(<http://iopscience.iop.org/0305-4470/33/30/313>)

View [the table of contents for this issue](#), or go to the [journal homepage](#) for more

Download details:

IP Address: 171.66.16.123

The article was downloaded on 02/06/2010 at 08:29

Please note that [terms and conditions apply](#).

Tunnelling coefficients across an arbitrary potential barrier

Aihua Zhang, Zhuangqi Cao, Qishun Shen, Xiaoming Dou and Yingli Chen

Molecular Photonics Laboratory, Institute of Optics and Photonics,
Shanghai JiaoTong University, Shanghai 200240, People's Republic of China

E-mail: ah.Zhang@yahoo.com

Received 7 March 2000, in final form 23 May 2000

Abstract. A simple, yet accurate, method of solving the Schrödinger equation across an arbitrary potential barrier is described, based on the analytic transfer-matrix technique. This paper gives the final analytical expression for the transmission probability. Numerical calculations for four typical potential barrier structures are compared with the traditional WKB, modified WKB and the modified Airy function (MAF) methods. Excellent agreement with an exact example is demonstrated. Most importantly, in cases where other potential-barrier methods fail, our method performs well.

Tunnelling in quantum-well and superlattice structures has recently attracted more interest, due to the development of high-speed and novel devices. A variety of approximate and numerical techniques for solving the Schrödinger equation have been developed [1–7]. However, a limited number of potentials can be solved analytically. Among the approximate approaches, the Wentzel–Kramos–Brillouin (WKB) method has been widely used due to its simple mathematical form and clear physical interpretation. Although it is restricted to slowly varying potential profiles that are continuous, many refinements have been developed to improve its accuracy, such as the modified conventional WKB method (MWKB) [4]. However, these also fail to provide perfect results. Using numerical methods, such as those based on the multistep potential approximation, one can obtain accurate solutions, but one tends to lose a great deal of physical insight in the process [2].

In this paper, we provide a general analysis of tunnelling across an arbitrary potential barrier and give a final analytical result with explicit physical meaning. We discuss the results obtained using our method for four typical profiles. The calculated tunnelling coefficients are compared with those obtained using WKB, MWKB, modified Airy functions (MAF) [5] and numerical methods. It is shown that our results agree well with exact numerical calculations. Numerical comparisons for several types of potential barrier show our method to succeed well where other potential-barrier methods, such as WKB, MWKB, MAF and even the improved MAF method [1], fail.

In the present calculation, rather than dealing with continuous variations of potential energy, we first divide the potential barrier into segments, in which the potential energy can be regarded as a constant $V(x_i)$. In the limit, as the divisions become finer and finer, a continuous variation will be recovered. An arbitrary potential barrier is shown in figure 1, where $x = 0$, x_s are the truncation points and x_c , x_t are turning points. E is the incident energy. We divide the regions $(0, x_c)$, (x_c, x_t) and (x_t, x_s) into l , m and n layers with equal width h , respectively.

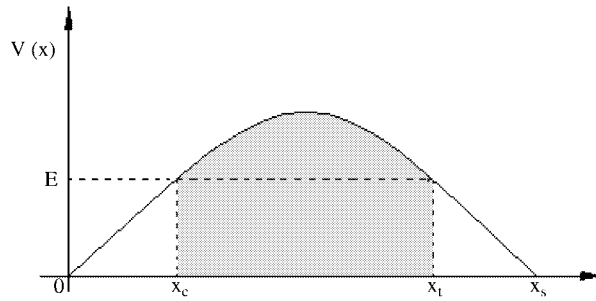


Figure 1. An arbitrary potential barrier.

As is well known, the field has an oscillatory character in the field $x < x_c$ and $x > x_t$, so the corresponding transfer matrix can be written as [8]

$$M_i = \begin{bmatrix} \cos(k_i h) & -\frac{1}{k_i} \sin(k_i h) \\ k_i \sin(k_i h) & \cos(k_i h) \end{bmatrix} \quad (i = 1, 2, \dots, l) \quad (1)$$

$$M_j = \begin{bmatrix} \cos(k_j h) & -\frac{1}{k_j} \sin(k_j h) \\ k_j \sin(k_j h) & \cos(k_j h) \end{bmatrix} \quad (j = l+m+1, l+m+2, \dots, l+m+n) \quad (2)$$

where $k_i = \sqrt{2m(E - V(x_i))}/\hbar$ and $k_j = \sqrt{2m(E - V(x_j))}/\hbar$.

In the region $x_c < x < x_t$, due to its evanescent character, the transfer matrix is changed to

$$M_q = \begin{bmatrix} \cosh(\alpha_q h) & -\frac{1}{\alpha_q} \sinh(\alpha_q h) \\ -\alpha_q \sinh(\alpha_q h) & \cosh(\alpha_q h) \end{bmatrix} \quad (q = l+1, l+2, \dots, l+m) \quad (3)$$

where $\alpha_q = \sqrt{2m(V(x_q) - E)}/\hbar$. Imposing the boundary condition at $x = 0$ and x_s , we obtain the matrix equation

$$\begin{bmatrix} \varphi(0) \\ \varphi'(0) \end{bmatrix} = \left(\prod_{i=1}^l M_i \right) \left(\prod_{q=l+1}^{l+m} M_q \right) \left(\prod_{j=l+m+1}^{l+m+n} M_j \right) \begin{bmatrix} \varphi(x_s) \\ \varphi'(x_s) \end{bmatrix} \quad (4)$$

where φ is the wavefunction and the prime in φ' denotes differentiation with respect to x . We assume that the field in $x < 0$ and $x > x_s$ is as follows:

$$\varphi(x) = \begin{cases} A_0 e^{ik_0 x} + B_0 e^{-ik_0 x} & x < 0 \\ C_s e^{ik_s x} & x > x_s \end{cases} \quad (5)$$

where $k_0 = \sqrt{2m(E - V(0))}/\hbar$ and $k_s = \sqrt{2m(E - V(x_s))}/\hbar$.

By using equation (5), equation (4) can be changed into

$$\left(-ik_0 \frac{A_0 - B_0}{A_0 + B_0}, 1 \right) \left(\prod_{i=1}^l M_i \right) \left(\prod_{q=l+1}^{l+m} M_q \right) \left(\prod_{j=l+m+1}^{l+m+n} M_j \right) \begin{pmatrix} 1 \\ ik_s \end{pmatrix} = 0. \quad (6)$$

After some simple algebraic manipulations we obtain

$$\left(-ik_0 \frac{A_0 - B_0}{A_0 + B_0}, 1\right) \prod_{i=1}^l M_i \prod_{q=l+1}^{l+m} M_q \begin{pmatrix} 1 \\ iK_t \end{pmatrix} = 0 \tag{7}$$

where $K_t = K_{l+m+1}$ and

$$iK_j = -k_j \tan\left(\tan^{-1}\left(\frac{K_{j+1}}{ik_j}\right) - k_j h\right) \quad (j = l + m + 1, \dots, l + m + n) \tag{8}$$

where $K_{l+m+n+1} = K_s$.

This means that the field solution beyond the turning point can be expressed, corresponding to (5), as

$$\varphi(x) = C_t e^{iK_t(x-x_t)} \quad (x > x_t). \tag{9}$$

With the same algebraic manipulation we can deduce the following equation from (7):

$$\left(-ik_0 \frac{A_0 - B_0}{A_0 + B_0}, 1\right) \begin{pmatrix} 1 \\ iK_1 \end{pmatrix} = 0 \tag{10}$$

where

$$iK_p = -k_p \tan\left(\tan^{-1}\left(\frac{K_{p+1}}{ik_p}\right) - k_p h\right) \tag{11}$$

$$k_p = \sqrt{2m(E - V(x_p))}/\hbar \quad (p = 1, 2, \dots, l, l + 1, l + 2, \dots, l + m).$$

In this calculation process we have used the identical equation identity

$$\cos(i\gamma h) = \cosh(\gamma h) \quad \sin(i\gamma h) = i \sinh(\gamma h). \tag{12}$$

Here we set

$$\phi_p = \tan^{-1}\left(\frac{K_p}{ik_p}\right). \tag{13}$$

Using equation (11) we can obtain

$$\begin{aligned} \phi_p &= m_p \pi + \tan^{-1}\left(\frac{K_{p+1}}{ik_p}\right) - k_p h \\ &= m_p \pi + \tan^{-1}\left(\frac{k_{p+1}}{k_p} \tan \phi_{p+1}\right) - k_p h \quad (p = 1, 2, \dots, l + m, m_p = 0, 1, \dots). \end{aligned} \tag{14}$$

In order to obtain an appropriate form which can give a clear physical insight, we proceed by writing equation (14) as follows:

$$k_p h + \left[\phi_{p+1} - \tan^{-1}\left(\frac{k_{p+1}}{k_p} \tan \phi_{p+1}\right)\right] = m_p \pi + \phi_{p+1} - \phi_p. \tag{15}$$

For $p = l + m$ we have

$$k_{l+m} h = m_{l+m} \pi + \tan^{-1}\left(\frac{K_t}{ik_{l+m}}\right) - \tan^{-1}\left(\frac{K_{l+m}}{ik_{l+m}}\right). \tag{16}$$

Summing over the index p , we have

$$\sum_{p=1}^{l+m} k_p h + \sum_{p=1}^{l+m-1} \left[\phi_{p+1} - \tan^{-1}\left(\frac{k_{p+1}}{k_p} \tan \phi_{p+1}\right)\right] = m_p \pi + \tan^{-1}\left(\frac{K_t}{ik_{l+m}}\right) - \tan^{-1}\left(\frac{K_1}{ik_1}\right). \tag{17}$$

In order to simplify the above equation, letting $(l + m) \rightarrow \infty$ and $h \rightarrow 0$ then $k_{l+m} \rightarrow 0$ and

$$\tan^{-1} \left(\frac{K_l}{ik_{l+m}} \right) \rightarrow \frac{1}{2}\pi$$

so we may write equation (17) as

$$\int_0^{x_t} k(x) dx + \xi = m_p \pi + \frac{1}{2}\pi - \tan^{-1} \left(\frac{K_1}{ik_1} \right) \tag{18}$$

where

$$\xi = \sum_{p=1}^{l+m-1} \left(\phi_{p+1} - \tan^{-1} \left(\frac{k_{p+1}}{k_p} \tan \phi_{p+1} \right) \right).$$

From (18) we obtain the following new conclusions.

- (a) It is clear that subscript p and $p + 1$ indicate the neighbouring section layer in the profile. If we let $k_{p+1} = k_p$, we have neglected the potential energy difference of the neighbouring section layers, and thus we obtain $\xi = 0$, so ξ can be interpreted as the phase contribution of the sub-waves reflected from every interface between the two neighbouring segments [8]. In most approximate methods ξ is neglected.
- (b) We integrate the $k(x)$ from the first truncating point x_0 to the second turning point x_t , whereas the WKB method uses the two turning points.
- (c) Note that the half-phase contribution at the turning points is $\pi/2$. This is totally different from the WKB method in which it is exactly equal to $\pi/4$.

From equation (10), we can obtain the reflection coefficient r ,

$$r = \frac{B_0}{A_0} = \frac{k_0 - K_1}{k_0 + K_1}. \tag{19}$$

Since $\tan \phi_1 = \frac{K_1}{ik_1}$, we therefore have

$$\frac{k_1 - K_1}{k_1 + K_1} = \exp(-2i\phi_1) = \exp\left(-2i \tan^{-1} \left(\frac{K_1}{ik_1} \right)\right). \tag{20}$$

With the condition $h \rightarrow 0$ we introduce the only approximation used in the calculation process: since x_1 is just close to the truncation points x_0 , and $V(x_0)$ is almost equal to $V(x_1)$, then $k_0 \approx k_1$.

According to (19) and (20), we obtain

$$r = \exp \left[2i \left(\int_0^{x_t} k(x) dx + \xi - \frac{1}{2}\pi + m_p \pi \right) \right]. \tag{21}$$

The tunnelling coefficient D is then expressed by

$$D = 1 - |r|^2 \tag{22}$$

where

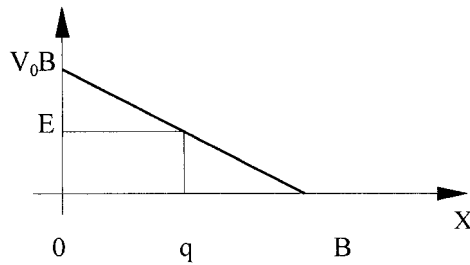
$$\begin{aligned} \xi &= \sum_{p=1}^{l+m-1} \left(\phi_{p+1} - \tan^{-1} \left(\frac{k_{p+1}}{k_p} \tan \phi_{p+1} \right) \right) \\ \phi_p &= \tan^{-1} \left(\frac{K_p}{ik_p} \right) \\ iK_p &= -k_p \tan \left(\tan^{-1} \left(\frac{K_{p+1}}{ik_p} \right) - k_p h \right) \\ k_p &= \sqrt{2m(E - V(x_p))}/\hbar \quad (p = 1, 2, \dots, l, l + 1, l + 2, \dots, l + m). \end{aligned}$$

In order to illustrate the accuracy of our method, we present here some typical results for the tunnelling coefficient obtained by the present theory, the WKB, MWKB, MAF and the exact numerical results. In our calculations we divide the whole potential into 500 and 5000 layers equally.

We have chosen a truncated linear step, a truncated exponential step, a truncated parabolic potential and a truncated quartic potential as our four examples [1].

Example 1: Truncated linear step potential:

$$V(X) = \begin{cases} 0 & X < 0 \\ V_0(B - X) & 0 < X < B \\ 0 & X > B. \end{cases}$$



In the following four profiles, $X = 0, B$ are the truncation points and $X = q, -q$ are the turning points.

$X = x/a$ and $B = b/a$ are both normalized, the Schrödinger equation can be written as

$$\frac{d^2\psi}{dx^2} + \alpha^2 \left[\varepsilon - \frac{V(X)}{V_0} \right] \psi = 0$$

where

$$k^2(x) = \alpha^2(\varepsilon - V(X)/V_0) \quad \alpha = (2ma^2V_0)^{1/2}/\hbar \quad \varepsilon = E/V_0.$$

In this paper we assume $\alpha = 1$ without any loss of generality. So in the linear step potential $k(X) = \varepsilon - V(X)/V_0 = \varepsilon - B + X$.

Table 1. Comparison of the variation of the tunnelling coefficient D with B . $B - \varepsilon = 0.5$ for the truncated linear step potential (example 1).

B	Numerical	Present (500)	Present (5000)	WKB	MWKB	MAF
3	0.6077	0.6059	0.6075	0.4670	0.6962	0.6078
6	0.4818	0.4784	0.4815	0.4670	0.5163	0.4856
8	0.4370	0.4325	0.4374	0.4670	0.4522	0.4377
15	0.3423	0.3353	0.3416	0.4670	0.3353	0.3431
20	0.3052	0.3139	0.3048	0.4670	0.2917	0.3050

Example 2: Truncated exponential step potential:

$$V(X) = \begin{cases} 0 & X < 0 \\ V_0 \exp(-X) & X > 0 \end{cases}$$

where $k(X) = \varepsilon - \exp(-X)$.

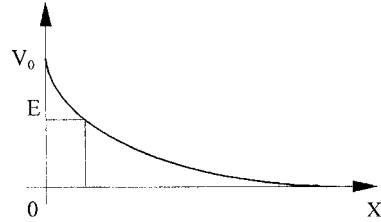


Table 2. Comparison of the tunnelling coefficient D for different values of ε for the truncated exponential step potential (example 2).

ε	Numerical	Present (500)	Present (5000)	WKB	MWKB	MAF
0.25	0.4789	0.4772	0.4788	0.2247	0.3892	0.4865
0.50	0.7549	0.7527	0.7549	0.4221	0.8443	0.7601
0.75	0.8702	0.8672	0.8695	0.5693	0.9861	0.8733

Example 3: Truncated parabolic potential:

$$V(X) = \begin{cases} = 0 & X < -B \\ = V_0(B^2 - X^2) & -B < X < B \\ = 0 & X > B \end{cases}$$

where $k(X) = \varepsilon - B^2 + X^2$.

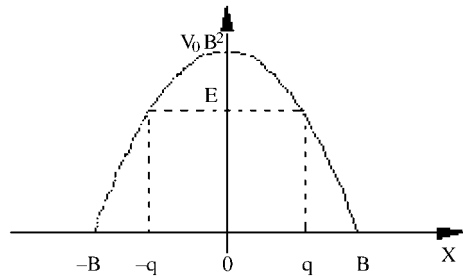


Table 3. Comparison of the tunnelling coefficient D for $B = 1$ for different values of ε for the truncated parabolic potential (example 3).

ε	Numerical	Present (500)	Present (5000)	WKB	MAF	MMAF
0.50	0.4604	0.4600	0.4603	0.1878	0.1003	0.3981
0.20	0.2141	0.2133	0.2141	0.0778	0.0506	0.1859
0.10	0.1124	0.1109	0.1122	0.0575	0.0390	0.0971

Example 4: Truncated quartic potential:

$$V(X) = \begin{cases} 0 & X < -B \\ V_0(B^4 - X^4) & -B < X < B \\ 0 & X > B \end{cases}$$

where $k(X) = \varepsilon - B^4 + X^4$.

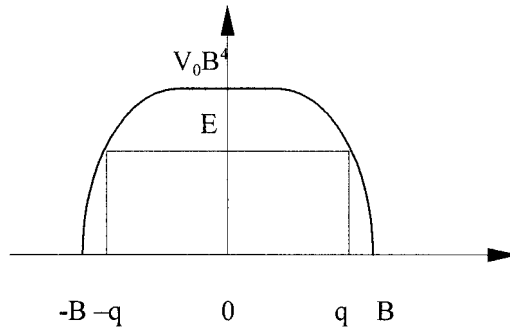


Table 4. Comparison of the tunnelling coefficient D for $B = 10$ of the truncated quartic potential (example 4).

$B^4 - \varepsilon$	Numerical	Present (500)	Present (5000)	MWKB	MAF
0.50	0.0741	0.06041	0.0743	0.1176	0.0709
1.00	0.0220	0.0178	0.0219	0.0299	0.0217

The above results clearly show that the present method produces much more accurate results than the other approximations.

From table 1, the MAF method is shown to have a similar accuracy to the numerical method. As we know, the MAF function is accurate for a linear potential but for the other potential barriers the MAF method is not as accurate as ours.

The method we have developed not only gives an analytical expression (21) for the tunnelling through an arbitrary one-dimensional potential barrier, but also much more accurate numerical results. Unlike the WKB solution, our method can hold throughout the region of interest, including at the turning points.

Acknowledgments

The authors acknowledge support from the National Natural Science Foundation of China, the MOST of China, the Novel Material Research Center of Shanghai and Shanghai Education Committee Foundation.

References

- [1] Roy S, Ghatak A K, Goyal I C and Gallawa R L 1993 Modified Airy function method for the analysis of tunneling problems in optical waveguides and quantum-well structures *IEEE J. Quantum Electron.* **29** 340–345
- [2] Ando Y and Itoh T 1987 Calculation of transmission tunneling current across arbitrary potential barriers *J. Appl. Phys.* **81** 1497–502

- [3] Ghatak A K and Lokanathan S 1984 *Quantum Mechanics: Theory and Applications* 3rd edn (New Delhi: Macmillan)
- [4] Love J D and Winkler C 1977 Attenuation and tunneling coefficients for leaky rays in multilayered optical waveguides *J. Opt. Soc. Am.* **67** 1627–33
- [5] Ghatak A K, Gallawa R L and Gayal I C 1992 Accurate solutions to Schrödinger's equation using modified Airy functions *IEEE J. Quantum Electron.* **28** 400–3
- [6] Nakamura K, Shimizu A and Koshiya M 1991 Finite-element calculation of the transmission probability and the resonant-tunneling lifetime through arbitrary potential barriers *IEEE J. Quantum Electron.* **27** 1189–98
- [7] Ghatak A K, Thyagarajan K and Shenoy M R 1987 Numerical analysis of planar optical waveguides using matrix approach *J. Lightwave Technol.* **5** 660–6
- [8] Cao Z, Jiang Y, Shen Q and Chen Y 1999 Exact analytical method of planar optical waveguides with arbitrary index profile *J. Opt. Soc. Am. A* **16** 2209–12